Chemico-Biological Interactions 254 (2016) 1–10

Contents lists available at ScienceDirect

Chemico-Biological Interactions

journal homepage: www.elsevier.com/locate/chembioint

The interaction of perfluorooctane sulfonate with hemoglobin: Influence on protein stability

Yanqing Wang [a, *], Hongmei Zhang [a], Yijun Kang [b], Zhenghao Fei [a], Jian Cao [a, **]

[a] Institute of Applied Chemistry and Environmental Engineering, Yancheng Teachers University, Yancheng City, Jiangsu Province, 224002, People's Republic of China

[b] College of Marine and Bio-engineering, Yancheng Teachers University, Yancheng City, Jiangsu Province, 224002, People's Republic of China

ARTICLE INFO

Article history:
Received 26 January 2016
Received in revised form
13 April 2016
Accepted 15 May 2016
Available online 17 May 2016

Keywords:
Perfluorooctane sulfonate
Hemoglobin
Binding interaction
Denaturation
Toxicological evaluation

ABSTRACT

Perfluorooctane sulfonate (PFOS) is among the most prominent xenobiotics contaminants in human blood. To evaluate the toxicity of PFOS at the protein level, the influences of PFOS on the stability and conformation of hemoglobin (Hb) has been investigated by circular dichroism (CD), UV–vis, and fluorescence spectroscopic methods and molecular modeling. CD spectral data indicated that the binding process of PFOS with Hb induced the relatively large changes in secondary structure of protein. Thermal denaturation of Hb, when carried out in the presence of PFOS, also indicated that PFOS acted as a structure destabilizer for protein. UV–vis, and fluorescence spectroscopic data indicated that the tertiary structures of Hb were also changed by PFOS binding. Hb did undergo significant changes in the heme group symmetry, implying that the functions of Hb could be disturbed by PFOS. In addition, molecular modeling study shows that PFOS could enter into the binding cavity of Hb by many noncovalent interactions. Overall, these data provide a mechanist explanation for the longer biological half-life of PFOS in human blood and provide useful information that could be associated with the toxicity of PFOS.

1. Introduction

Perfluorinated chemicals (PFCs) are man-made fluorinated hydrocarbons, which are widely detected groups of organic compounds in the environment and generate great health concerns [1]. Now, PFCs are widely used in the manufacture of a variety of products, such as food packaging, floor waxes, polymeric products, and industrial surfactant because of the outstanding chemical properties of them [2,3]. Among of PFCs, perfluorooctane sulfonate (PFOS) is the most common monomers and can be found in the environment, including marine and terrestrial animals at ng g^{-1} level [4]. Even in humans, PFOS was detectable in breast milk and blood plasma at ng mL^{-1} levels [5]. According to the EFSA opinion the fish and seafood (50–80%), fruit and fruit products (8–27%) and meat and meat products (5–8%) contributed to PFOS exposure in diet [6]. Although PFOS is detected at very low levels in the environment, it can reach high concentrations in blood plasma of wildlife and humans because of its low degradation, high bioaccumulation, and long-range transport capacity [7]. The toxicity, mobility and bioaccumulation potential of PFOS pose potential adverse effects for the environment and human health [7]. PFOS concentration in human blood, ranges 14–59 ng/ml, around the world, and it was eliminated in serum for 5.4 year [8]. Therefore, PFOS was identified as a priority hazardous substance according to the European Directive 2013/39/EU, in the field of water policy in the recent years [9]. Pharmacokinetic and pharmacodynamic studies shows that half-lives of PFOS have been established in 1–2 months, 4 months, and 4.8 years in rodents, monkeys, and humans, respectively [10]. In addition, PFOS could disturb homeostasis of N9 cells, impact mitochondria, and affect gene expression of apoptotic regulators [11]. Although toxicology studies have revealed that PFOS can cause a diversity of adverse effects on living organisms, the underlying toxic mechanisms are still not well known [12]. Because of the hydrophobic group and the polar end, perfluorinated chemicals have great potential to cross membranes and enter red blood cells [13].

Hemoglobin (Hb) is a kind of respiratory protein in red blood cell [14]. Its mechanisms of carrying oxygen and transferring electron, enzymatic and antioxidant activities had been realized [15,16]. For the purpose of investigation about the biocompatibility

* Corresponding author.
** Corresponding author.
E-mail addresses: wyqing76@126.com (Y. Wang), yctu_caojian@126.com (J. Cao).

http://dx.doi.org/10.1016/j.cbi.2016.05.019
0009-2797/

and toxicity of PFOS, the fundamental understandings of the conformational and functional behaviors of Hb in the presence of PFOS are of critical importance for the integration of the transport and metabolism process of PFOS. Many studies have been made concerning the interactions of hemoglobin with various classes of molecules such as drugs [17] and toxic molecule [18,19], but also with surfactants [20,21], polymers [22] and nanoparticles [23,24]. Recently, R.T. Liu et al. have studied the binding interaction of perfluorodecanoic acid with hemoproteins [25]. However, in my knowledge, the present study is the first one concerning the interaction between PFOS and hemoglobin.

Herein, we used circular dichroism (CD), fluorescence, UV/vis absorption spectra techniques and molecular modeling method to study the binding mechanism of PFOS with Hb. Effects of PFOS on the thermal stability and conformational structure of Hb were also studied to obtain the nature of their binding interactions. The studies on the binding mechanism of PFOS with Hb can provide the basic data including the thermal stability and conformational structure changes of Hb by PFOS for understanding the toxicity mechanism of PFOS in vivo.

2. Material and methods

2.1. Apparatus and reagents

The fluorescence spectra were recorded on LS–50B spectrofluorimeter (Perkin–Elmer USA). The UV/vis spectra were recorded on a SPECORD S600 (Jena, Germany) and the CD spectra were measured by a Chirascan spectrometer (Applied Photophysics Ltd., Leatherhead, Surrey, UK).

Bovine hemoglobin (BHb) was purchased from Sigma–Aldrich Chemical Company and used without further purification. PFOS was purchased from Aladdin Industrial Corporation. The other chemicals were all of analytical purity. The PFOS (0.05 mol/L) was prepared in Methanol. Hb solution (5.0×10^{-6} mol/L) was prepared in pH 7.40 phosphate buffer. Doubly distilled water was used throughout.

2.2. Spectral measurements

All fluorescence spectra were measured with the excitation at 280 nm and the emission wavelengths at 300–500 nm with 5.0 nm/5.0 nm slit widths. A 2.5 mL portion of a 5.0×10^{-6} mol/L solution of Hb was titrated manually by successive additions of PFOS solution. The synchronous fluorescence spectra of Hb in the absence and presence of PFOS were recorded with the $\Delta\lambda$ values of 15 nm or 60 nm. In addition, for three-dimensional fluorescence spectra, the emission wavelengths range was selected from 270 to 500 nm, the initial excitation wavelength was set from 200 to 340 nm with increments of 10 nm.

The UV/vis absorbance spectra of Hb and Hb-PFOS system were recorded under the following conditions: wavelength 200–800 nm, slit width 1 nm and scanning speed 50 nm/min.

For the CD experiments, a 0.02 mol/L phosphate buffer of pH 7.40 was exclusively prepared in ultrapure water. The 5.0×10^{-6} mol/L Hb solution in presence and absence of PFOS were recorded from 200 to 260 nm with three scans averaged and scanning speed was set at 30 nm/min for each CD spectrum. The circular dichroism neural networks software (CDNN) was used to analyze CD spectra. The temperature of thermal denaturation of Hb in the absence and presence of PFOS was varied from 20 to 90 °C in 5 °C steps, with 240 s increments. The melting temperature (T_m) and the enthalpy changes at the melting temperature (ΔH_m) of Hb were obtained by using the Global Analysis Software. In addition, the scanning range from 390 to 500 nm were used to study the effect of PFOS on heme spectra of Hb.

2.3. Molecular docking simulation

The docking study was performed with Autodock 4.2.3 software obtained from the Scripps Research Institute [26]. The structure of Hb (PDB ID 1G09) was taken from RCSB Protein Data Bank [27]. PFOS was optimized by using Gaussian 09 at DFT/B3LYP/6-311++G level [28]. During the modeling docking study, a grid box of 126–126–126 with spacing of 0.700 Å was used in order to include all possible binding sites for PFOS on Hb. The maximum number of energy evaluation was set at 2,500,000, GA population size was set at 150, and the number of GA runs were set at 100. Finally, the best docking results were further analyzed by using the Molegro Molecular Viewer software (Molegro-a CLC bio company, Aarhus, Denmark) [29].

3. Results and discussion

3.1. Secondary structure changes shown by CD spectra

In the present work, circular dichroism (CD) spectral method was used to analyze the effect of PFOS on the conformation and thermal stability of Hb. Fig. 1(A, B) shows the far-UV CD spectra of Hb in the absence and presence of different concentrations of PFOS. As shown in Fig. 1(A), the spectrum of Hb has an intense positive peak at about 197 nm and two negative bands at 208 nm and 222 nm, characteristic of the α-helical structure. It can be seen that the intensities of the negative bands at 208 nm and 222 nm

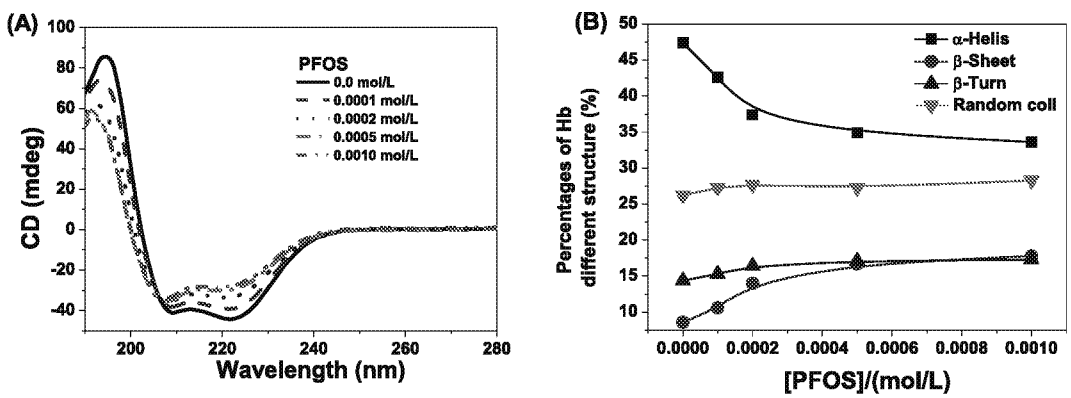

Fig. 1. (A) Effect of PFOS on the CD spectrum of Hb (5.0×10^{-6} mol/L). (B) Plots of the percentages of the different structures of Hb in the absence and presence of PFOS.

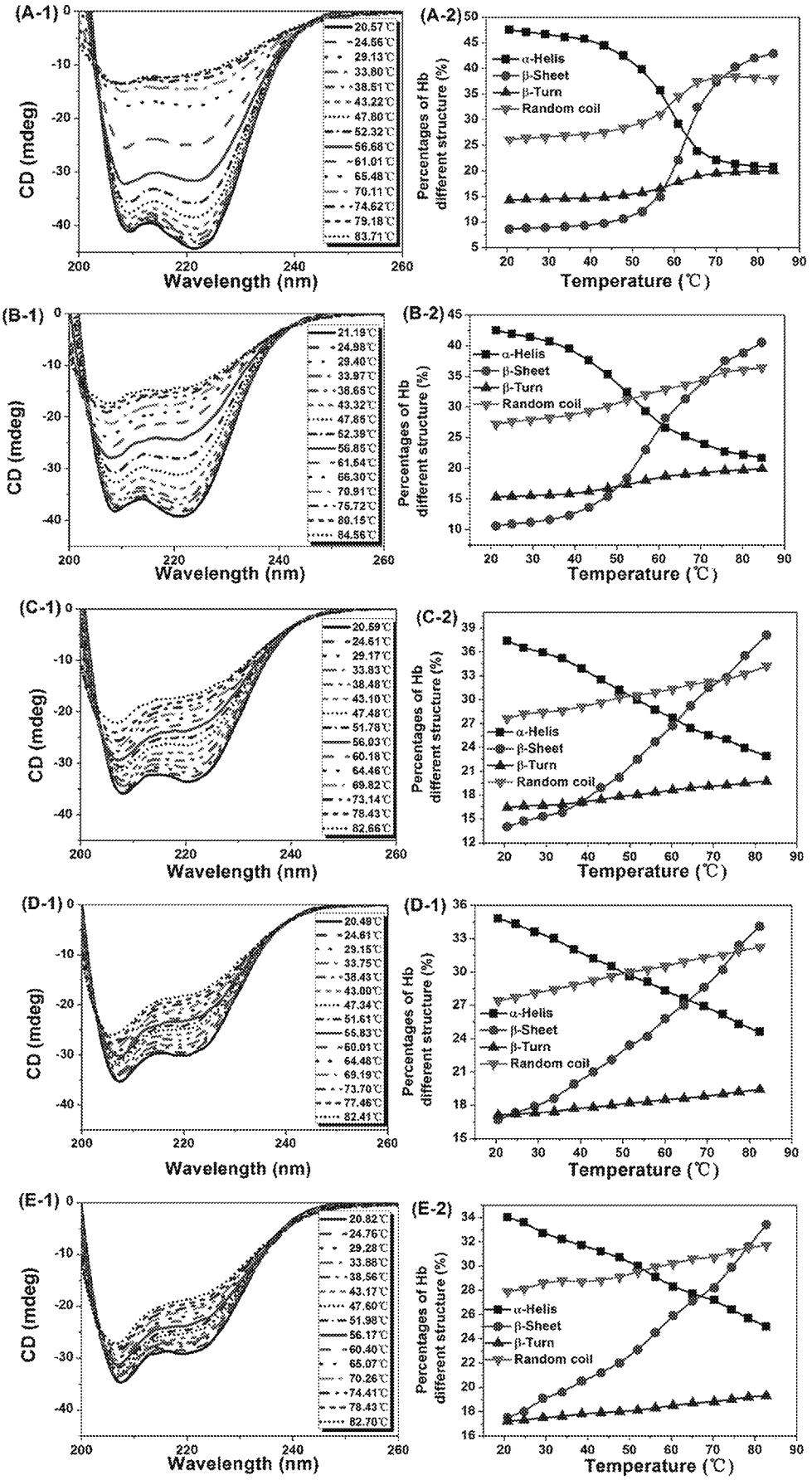

Fig. 2. (A-1, B-1, C-1, D-1, E-1) Far-UV CD spectra of Hb (5.0×10^{-6} mol/L) at different temperature in the absence and presence of different concentration of PFOS, (A-2, B-2, C-2, D-2, E-2) Plots of the percentages of the different structures of Hb at different temperature in the absence and presence of PFOS. c (PFOS): A, 0.0000 mol/L, B, 0.0001 mol/L, B 0.0002 mol/L, 0.0005 mol/L, 0.0010 mol/L.

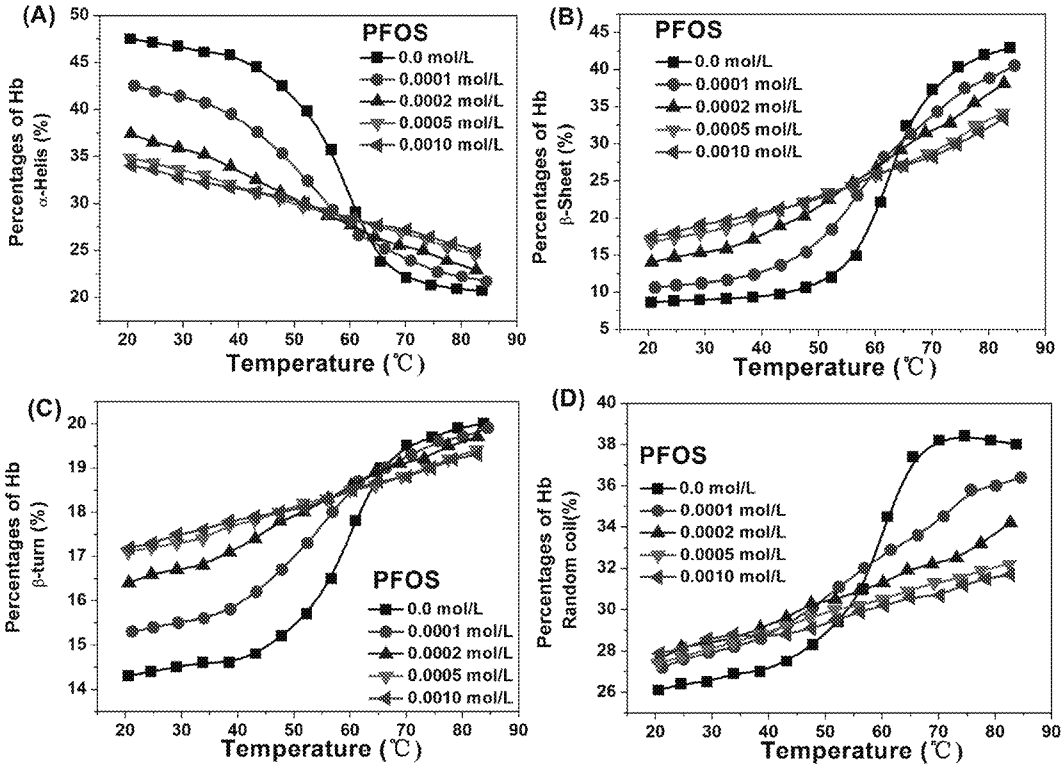

Fig. 3. The representative illustrations of the second structural content at different temperature in the presence of different PFOS concentrations. A, α-helix; B, β-sheet; C, β-turn; D, random coil.

increased and that of positive peak at about 197 nm decreased with addition of PFOS. In addition, the peaks at 208 nm and 197 nm exhibit a slight blue shift, showing that the binding interaction of PFOS with Hb induced the relatively large changes in secondary structure and probably some changes in the tertiary structure of protein [30,31]. The secondary structural percentages of α-Helix, β-Sheet, β-Turn and Random coil in Hb with the increase of PFOS concentrations were plotted in Fig. 1(B). It can be seen from the figures that the proportion of α-Helix decreased from 47.4% in free Hb to 33.6% with the increase of PFOS concentration. In addition, the amount of β-Sheet increased from 8.6% in free Hb to 17.8% in the presence of PFOS. Very strong changes in the protein structures from α-Helix to β-Sheet clearly indicated that PFOS combined with the amino acid residues of the main polypeptide chain of Hb and induced the denaturation and unfolding of protein.

Herein, CD spectroscopy was also used to characterize the impact of above thermal denaturation on the secondary structure and unfolding transition of Hb. As Fig. 2 A-1,2 show, when the temperature increased, the content of α-helix decreased to 20% at about 90 °C, while the content of β-sheet and random coil increased. In addition, the changes in the second structural content against temperature is quite sharp when the temperature is beyond 43 °C, indicating that high temperature can easily unfold the α-Helix structure of Hb.

Compared with the thermal denaturation process of Hb in the absence of PFOS, the change trend in the same process of Hb-PFOS system shows some obvious changes (Fig. 2 B–E). For example, the changing trend of the α-helix content against temperature of Hb in the presence of PFOS decreased linearly, while those of β-sheet, β-turn and random coil increased linearly. This result implied that the presence of PFOS had an enormous capacity for changing the thermal denaturation process of Hb. In addition, the representative illustrations of the second structural content at different temperature in the presence of different PFOS concentrations was shown in Fig. 3(A–D). The results indicate that the protein in presence of PFOS is more prone towards thermal denaturation.

In order to gain a deep insight into the unfolding transition of Hb, Global Analysis Software was used to obtain the melting temperature (T_m) and the enthalpy changes at the melting temperature (ΔH_m). The results are listed in Table 1. It can be seen that T_m of Hb in the presence of PFOS was reduced from 59.2 °C to 53.0 °C, indicating that the thermal stability of Hb decreased and PFOS acted as a structure destabilizer. The observed decreasing trend of T_m in the presence of PFOS maybe results from a preferential interaction of PFOS with the thermally unfolded forms of Hb, shifting the folding to unfolding transition towards the forward direction [32]. In addition, the process of effect of temperature on protein often follows multiple steps: native (N)→extended (E)→unfolded (U) [32]. It is known that solvent plays a critical role in protein folding [33]and the ordering of water molecules around exposed the hydrophobic groups of folded protein play an important role in the thermal change of protein [34]. PFOS binding on Hb

Table 1
The melting temperature (T_m) and the enthalpy changes at the melting temperature (ΔH_m) of PFOS-Hb system.

System	T_m/°C	ΔH_m/(kJ/mol)
Hb	59.2 ± 0.1	182.1 ± 1.5
Hb + PFOS c (PFOS) = 0.0001 mol/L	55.0 ± 0.1	109.4 ± 1.1
Hb + PFOS c (PFOS) = 0.0002 mol/L	54.1 ± 0.3	148.9 ± 5.4
Hb + PFOS c (PFOS) = 0.0005 mol/L	53.8 ± 0.3	146.8 ± 5.2
Hb + PFOS c (PFOS) = 0.0010 mol/L	53.0 ± 0.2	146.5 ± 3.7

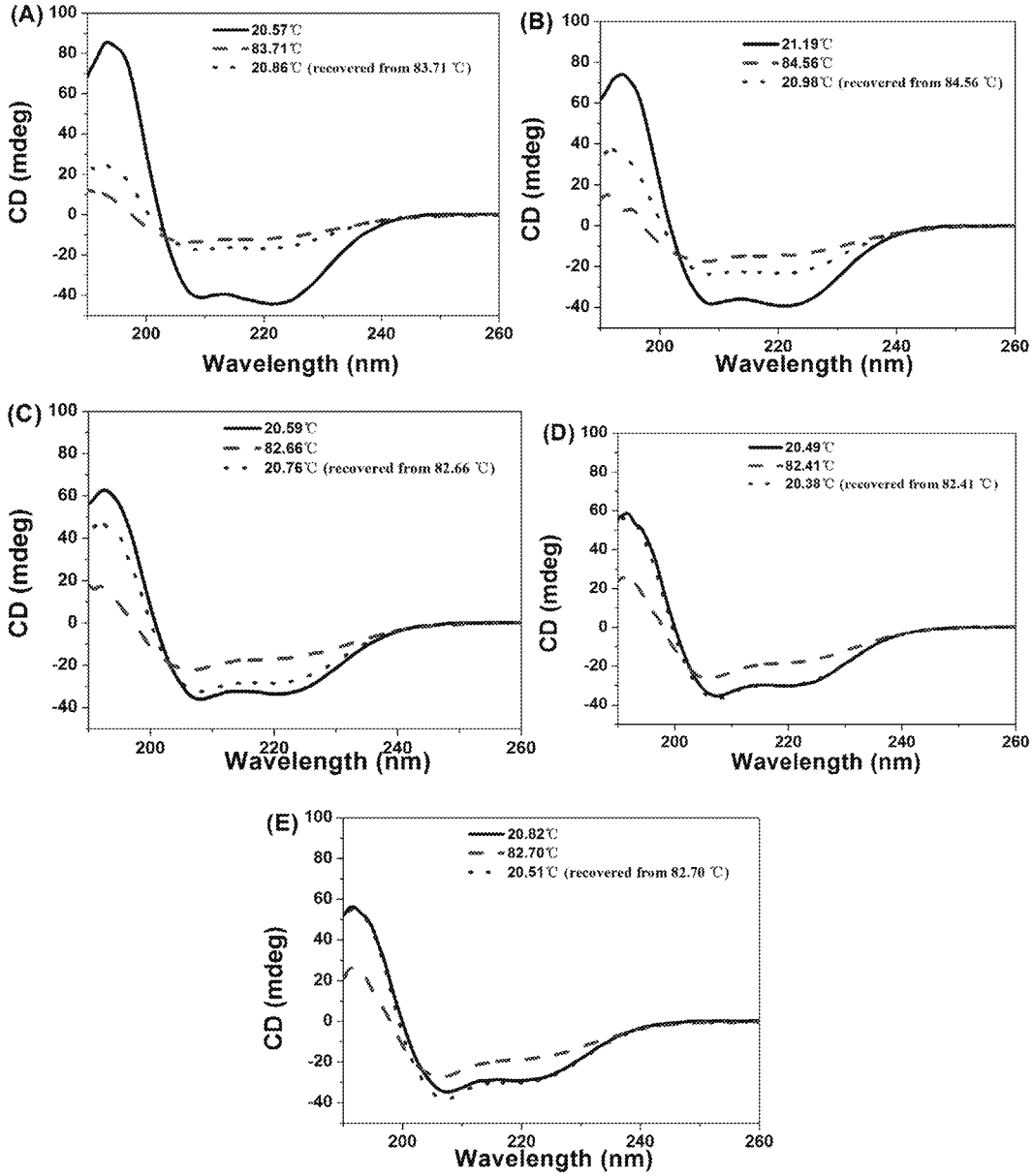

Fig. 4. CD spectra of Hb at different temperature in the absence (A) and presence (B–E) of PFOS at different conditions. c (Hb) = 5.0×10^{-6} mol/L, c (PFOS): A, 0.0000 mol/L, B, 0.0001 mol/L, B 0.0002 mol/L, 0.0005 mol/L, 0.0010 mol/L.

Table 2
Percentages of α-Helix structures of Hb and HB-PFOS at different temperature.

System	Temperature	α-Helix %
Hb	20.57 °C	47.5
	83.71 °C	20.7
	20.86 °C (recovered from 83.71 °C)	23.9
Hb + PFOS	21.19 °C	42.5
c (PFOS) = 0.0001 mol/L	84.56 °C	21.7
	20.98 °C (recovered from 84.56 °C)	27.8
Hb + PFOS	20.59 °C	37.4
c (PFOS) = 0.0002 mol/L	82.06 °C	22.9
	20.76 °C (recovered from 82.06 °C)	32.1
Hb + PFOS	20.49 °C	34.8
c (PFOS) = 0.0005 mol/L	82.41 °C	24.6
	20.38 °C (recovered from 82.41 °C)	34.4
Hb + PFOS	20.82 °C	34.0
c (PFOS) = 0.0010 mol/L	82.70 °C	25.0
	20.51 °C (recovered from 82.70 °C)	34.8

induces the loss of ordered water coating the peptide of Hb and makes the native state energetically less stable. The distance between –NH and –C=O groups of Hb are changed and the H-bonds of the backbone of Hb are broken. The hydrophobic side chains of Hb get exposed during the unfolding process to interact with the hydrophobic chain of PFOS, which results in the decrease of enthalpy change (ΔH_m).

From above CD analysis, we found that PFOS induced the denaturation and unfolding of Hb and affected the thermal denaturation process of protein. The native (N)→extended (E) is reversible whereas for the extended (E) →unfolded (U) transition the native state could not be retrieved upon decreasing the temperature [32]. The formation of complex between PFOS and Hb maybe affects the reversibility of the unfolding process when the protein is cooled from high temperature to 20 °C. It can be seen from Fig. 4(A) and Table 2 that the percentage of Hb the α-Helix changed from 47.5% to 20.7% when Hb was heated from 20.57 °C to

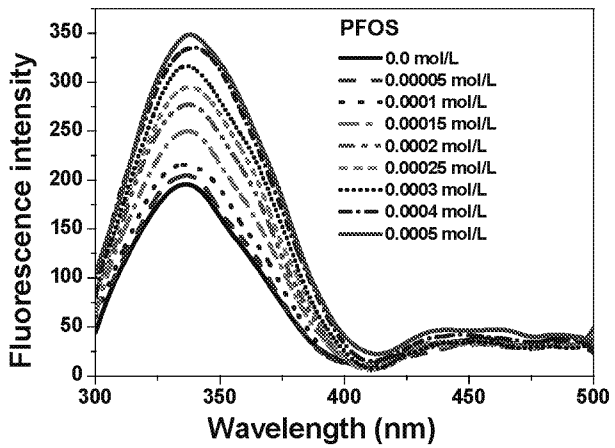

Fig. 5. Effect of PFOS on the fluorescence intensity of Hb, c (Hb) = 5.0×10^{-6} mol/L, pH = 7.40, T = 298 K.

3.2. Tertiary conformational changes shown by fluorescence spectra

The steady-state fluorescence spectra of Hb in the absence and presence of PFOS are shown in Fig. 5. Although Hb have six Trp residues, Hb exhibits a low fluorescence in water because the efficient energy transfer from Trp to heme significantly quenches the protein fluorescence [35,36]. As the result indicated, the fluorescence intensity of Hb is increased gradually with increasing of PFOS concentration. PFOS is a surfactant with a hydrophobic carbon chain and a hydrophilic sulfonate group. The hydrophobic chain in PFOS molecule not only is more like to interact with the hydrophobic amino residues in Hb, but also penetrate into the hydrophobic heme cavity. According to the Ref [25], perfluorooctanoic acid (PFOA) has little effect on the fluorescence intensity of hemoglobin. Therefore, the sulfonate group plays an important role in the binding interaction of PFOS with Hb. The increase of fluorescence intensity of Hb implies that the binding of PFOS to Hb is much stronger than that of PFOA. In other word, PFOS could pose more of

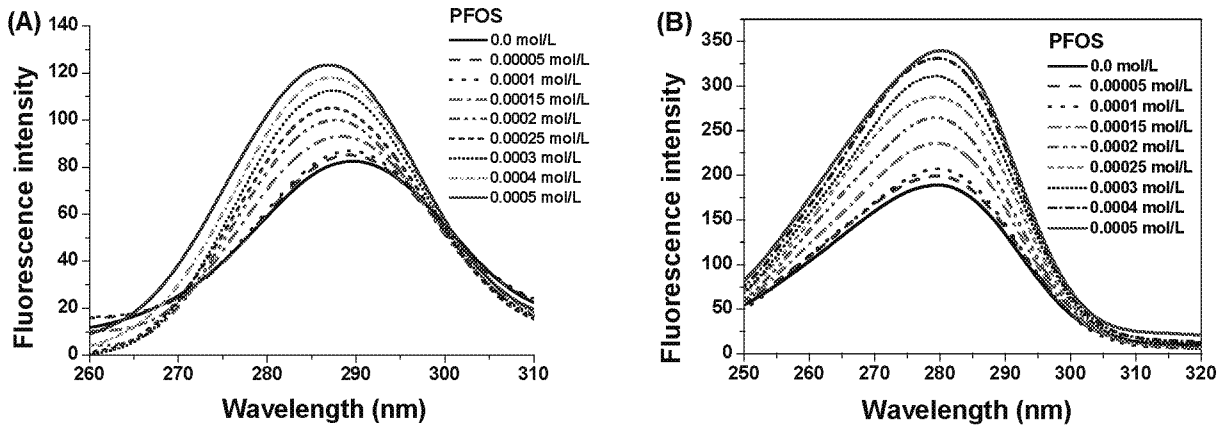

Fig. 6. Effects of PFOS on the synchronous fluorescence spectra of Hb, c (Hb) = 5.0×10^{-6} mol L^{-1}, pH = 7.40, T = 298 K (A, $\Delta\lambda$ = 15 nm; B, $\Delta\lambda$ = 60 nm).

83.71 °C. The α-Helix of 20.7% indicated that 119 amino acid residues (574 total residues × 0.207) are still maintained α-Helix at 83.71 °C. In addition, which α-Helix recovers to 23.9% as Hb solution is cooled down to 20.86 °C. This result indicated that Hb can only recover 3.2% of its α-Helix when the protein was cooled from 83.71 °C to 20.86 °C. This phenomenon implied that the structures of 18 amino acid residues (574 total residues × (0.239−0.207)) recovered from unfolding to α-Helix and only about 50% (137/helical 272 residues) of the original helices still have α-Helix when we cooled the protein from 83.71 °C to 20.86 °C. At high temperature, Hb obviously loses the reversibility of the structural change in the thermal denaturation. However, compared with the percentage of Hb α-Helix structures in absence of PFOS, Hb can recover more α-Helix when the temperature were cooled to about 20 °C. This implied that Hb-PFOS system have better reversibility of the structural change in the thermal denaturation than only Hb. The possible binding forces in the formation of the complex between PFOS and Hb might cause the observed increase in the reversibility of the unfolding process when the protein is cooled from high temperature to 20 °C. In the formation of the molecular structure of Hb-PFOS complex, the electrostatic interactions between the protonated $-SO^{3}-$ of PFOS and the $-NH3^{+}$ groups in Hb probably drives the binding of PFOS to Hb. In addition, the hydrophobic force between the hydrophobic carbon chain of PFOS and hydrophobic peptides should not be excluded.

a health threat than PFOA.

Generally, synchronous fluorescence spectroscopy has been widely used to separate out the emission peaks as well as to investigate the changes in the microenvironment of Tyr and Trp residues in protein [37]. The synchronous fluorescence spectra of Tyr and Trp residues in Hb were obtained by setting $\Delta\lambda$ = 15 and 60 nm, respectively. The effects of PFOS on the synchronous fluorescence spectra of Hb are shown in Fig. 6 (A, B). As the data indicated, the fluorescence of Tyr and Trp residues in Hb both exhibit a great enhancement upon the addition of PFOS. Fig. 7(A) shows the normalized fluorescence intensity of Hb at the maximum emission wavelength in the presence of different concentrations of PFOS. It can be seen that the fluorescence intensity of Tyr and Trp residues of Hb in the presence of PFOS were 1.455 and 1.797 times those of Tyr and Trp residues of Hb in the absence of PFOS, respectively. This phenomenon confirmed that Hb undergoes conformational changes in the presence of PFOS. In addition, the maximum emission peak of Tyr and Trp in Hb were also shown in Fig. 7(B). It is apparent from Fig. 7(B) that the emission peak of Tyr shows an obviously blue shift upon addition of PFOS. Compared with Tyr residues, the maximum emission wavelengths of Trp residues did not show obviously shift. These results further expresses the conformational changes of Hb, the polarity around Tyr residues is decreased and the hydrophobicity is increased [31]. In addition, the binding of PFOS to Hb did not obviously perturb the

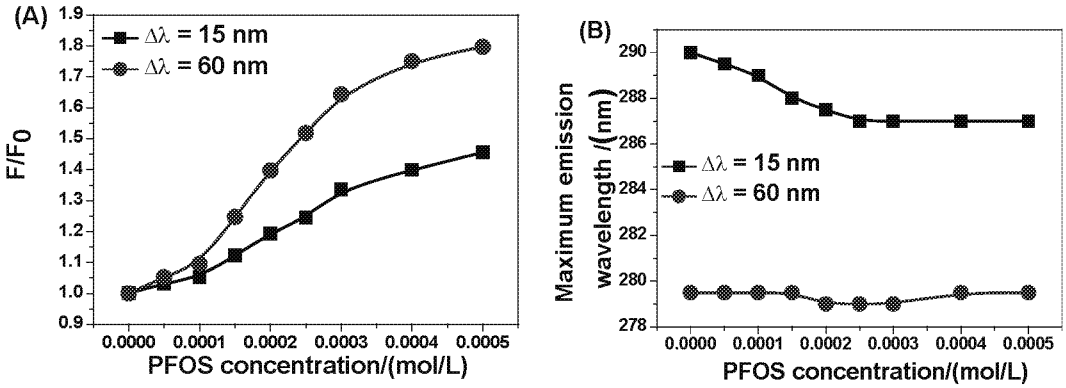

Fig. 7. Normalized fluorescence intensity of Hb at the maximum emission wavelength in the presence of different concentrations of PFOS (A); the maximum emission wavelength of Hb in the presence of different concentrations of PFOS (B). c (Hb) = 5.0×10^{-6} mol/L, pH = 7.40, T = 298 K (A, Δλ = 15 nm; B, Δλ = 60 nm).

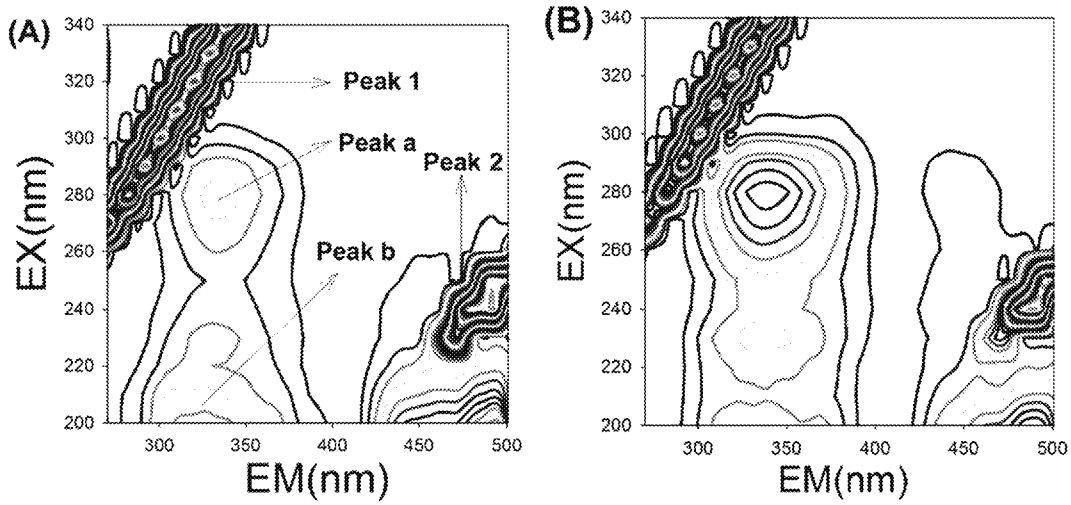

Fig. 8. The three–dimensional fluorescence spectral contours of Hb (A) and Hb-PFOS system (B). c (Hb): A, 5.0×10^{-6} mol/L, B, 5.0×10^{-6} mol/L; c (PFOS): A, 0.0×10^{-6} mol/L, B, 400.0×10^{-6} mol/L.

environment of Trp residues in Hb.

Herein, the three-dimensional Ex/Em fluorescence spectral method was used to visualize the excitation and emission maxima of the fluorophores in Hb. The three-dimensional fluorescence spectral contours of Hb and Hb-PFOS are shown in Fig. 8. It could be seen from Fig. 8(A) that there were two kinds of fluorescence spectral peaks including the Raleigh scattering peaks (Peak 1 and Peak 2) and endogenous fluorophores peaks (Peak a and Peak b). The endogenous fluorophores peaks of protein are highly sensitive to the local environment. Among them, peak a is caused by the $\pi \rightarrow \pi^*$ transition of aromatic amino acids in Hb and peak b is caused by the $n \rightarrow \pi^*$ transition of Hb's characteristic polypeptide backbone structure C=O [38]. Upon addition of PFOS to Hb solution, some remarkable changes of Peak a and Peak b were observed. Firstly, the increase of the stitch density of peak a, b indicated that the binding interaction of PFOS with Hb result in the fluorescence enhancement of endogenous fluorophores in Hb, which implied that PFOS can induce denaturalization of Hb. Secondly, the obviously changes of peak b indicated the secondary and tertiary structure changes of Hb.

3.3. Heme group region changes shown by UV–vis and CD spectra

The UV–vis spectra of Hb in the absence and presence of PFOS are shown in Fig. 9. It can be seen from this figure that, after the addition of PFOS, the UV–vis spectra of Hb show some interesting changes as follow. Firstly, a significant decrease of absorption in the

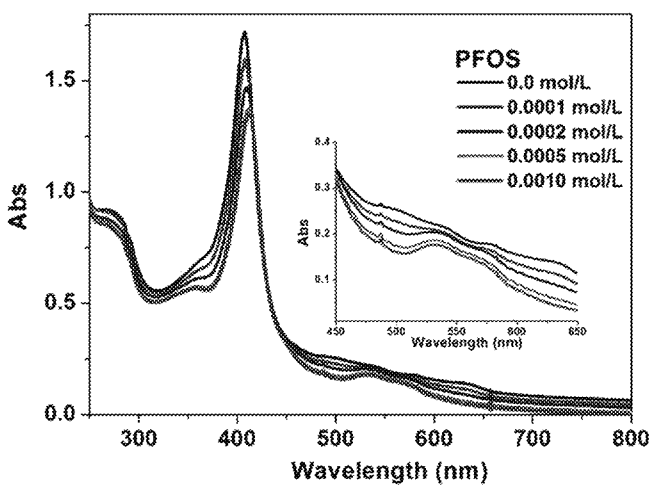

Fig. 9. Effect of PFOS on the UV–vis spectra of Hb (5.0×10^{-6} mol/L) in the absence and presence of PFOS.

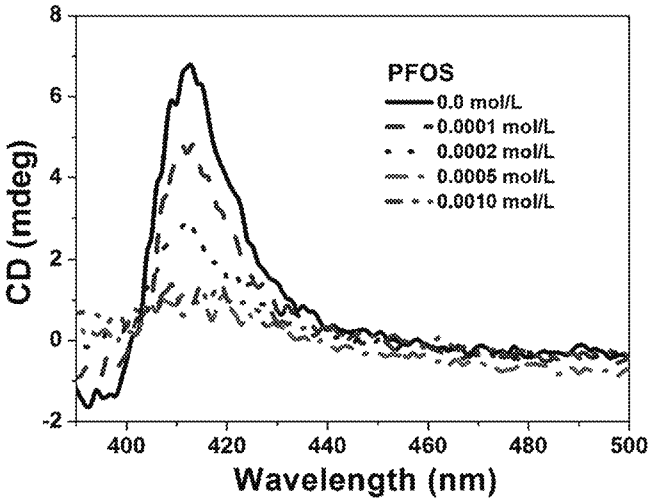

Fig. 10. Effect of PFOS on the CD spectra of Hb (5.0×10^{-6} mol/L) in the absence and presence of PFOS.

heme group region named the Soret band at about 408 nm and a red shift to 413 nm were observed in Fig. 9. Secondly, the absorption peaks at 576 nm and 627 nm disappears while a new one at 529 nm came in being. These spectral changes confirmed that PFOS could induce structural changes of Hb and result in decreasing the ability of Hb to bind to oxygen [25]. PFOS could penetrate into the heme pocket and disturb the hydrophobic balance of the heme cavity in Hb. These bands lie in a regions from 350 to 700 nm where only heme-associated electronic transitions are to be a dominant contributor. These changes at 408, 576, and 627 nm of Hb in the presence of PFOS signified a conformational changes of Hb at the tertiary state. Thus, the normal biological function of hemoprotein in transferring oxygen is effected by the binding interaction of PFOS with Hb [15]. In addition, the aromatic peak at 270 nm decreased and the peak obviously blue shifted, indicating that an alteration of the microenvironment of the aromatic residues in Hb. In accordance with fluorescence spectral data, the tertiary conformation of Hb was affected by PFOS. In order to confirm the Soret band change induced by PFOS, CD spectral method was also used in this work.

In Fig. 10 the CD spectra of Hb in the absence and presence of PFOS were shown. The Hb CD spectrum in the heme group region was characterized by main peak at 410 nm with positive ellipticity, which is associated to the heme group signal [39]. As the result

Table 3
Docking results of Hb with PFOS by using Autodock program generated different ligand conformations.

Rank	ΔG (kcal/mol)	$E_{\text{inter-mol}}$ (kcal/mol)	E_{VHD} (kcal/mol)	E_{elec} (kcal/mol)	E_{total} (kcal/mol)	$E_{\text{torsional}}$ (kcal/mol)	E_{unbound} (kcal/mol)
1	−3.38	−5.77	−3.05	−2.72	+0.72	+2.39	+0.72
2	−3.20	−5.58	−2.81	−2.77	+0.65	+2.39	+0.65
3	−3.16	−5.55	−3.17	−2.37	+0.50	+2.39	+0.50
4	−3.12	−5.50	−2.35	−3.15	+0.36	+2.39	+0.36
5	−3.07	−5.45	−2.89	−2.56	+0.57	+2.39	+0.57
6	−3.00	−5.39	−2.59	−2.81	+0.45	+2.39	+0.45
7	−2.96	−5.35	−2.62	−2.73	+0.31	+2.39	+0.31
8	−2.91	−5.30	−2.69	−2.61	+0.28	+2.39	+0.28
9	−2.82	−5.20	−2.49	−2.71	+0.38	+2.39	+0.38
10	−2.74	−5.13	−2.09	−3.04	+0.22	+2.39	+0.22
11	−2.72	−5.11	−2.41	−2.70	+0.33	+2.39	+0.33
12	−2.69	−5.08	−2.73	−2.34	+0.57	+2.39	+0.57
13	−2.68	−5.06	−2.20	−2.87	+0.70	+2.39	+0.70
14	−2.62	−5.01	−2.39	−2.62	+0.37	+2.39	+0.37
15	−2.61	−5.00	−2.13	−2.86	+0.36	+2.39	+0.36
16	−2.57	−4.96	−2.53	−2.43	+0.36	+2.39	+0.36
17	−2.44	−4.82	−3.36	−1.46	+0.49	+2.39	+0.49
18	−2.43	−4.81	−2.21	−2.60	+0.69	+2.39	+0.69
19	−2.35	−4.73	−3.64	−1.10	+0.27	+2.39	+0.27
20	−2.29	−4.68	−3.27	−1.41	+0.37	+2.39	+0.37
21	−2.22	−4.60	−1.78	−2.82	+0.44	+2.39	+0.44
22	−2.19	−4.57	−1.78	−2.79	+0.15	+2.39	+0.15
23	−2.16	−4.54	−1.90	−2.65	+0.20	+2.39	+0.20
24	−2.06	−4.45	−2.76	−1.69	+0.20	+2.39	+0.20
25	−2.06	−4.44	−1.72	−2.72	+0.41	+2.39	+0.41
26	−1.91	−4.30	−2.92	−1.38	+0.49	+2.39	+0.49
27	−1.84	−4.23	−2.71	−1.52	+0.53	+2.39	+0.53
28	−1.81	−4.19	−1.56	−2.63	+0.16	+2.39	+0.16
29	−1.79	−4.18	−2.92	−1.26	+0.18	+2.39	+0.18
30	−1.77	−4.16	−1.10	−3.06	+0.21	+2.39	+0.21
31	−1.71	−4.10	−2.18	−1.91	+0.13	+2.39	+0.13
32	−1.70	−4.09	−2.53	−1.55	+0.50	+2.39	+0.50
33	−1.60	−3.98	−2.35	−1.64	+0.43	+2.39	+0.43
34	−1.59	−3.97	−1.93	−2.05	+0.47	+2.39	+0.47
35	−1.53	−3.91	−2.49	−1.43	+0.32	+2.39	+0.32
36	−1.48	−3.87	−1.85	−2.02	+0.24	+2.39	+0.24
37	−1.47	−3.85	−2.32	−1.53	+0.50	+2.39	+0.50
38	−1.46	−3.85	−1.78	−2.07	+0.35	+2.39	+0.35
39	−1.40	−3.78	−2.71	−1.07	+0.64	+2.39	+0.64
40	−1.39	−3.78	−2.41	−1.37	+0.22	+2.39	+0.22
41	−1.38	−3.77	−2.13	−1.64	+0.53	+2.39	+0.53
42	−1.27	−3.65	−2.72	−0.94	+0.42	+2.39	+0.42
43	−1.21	−3.60	−2.32	−1.27	+0.40	+2.39	+0.40
44	−0.75	−3.14	−2.03	−1.10	+0.10	+2.39	+0.10

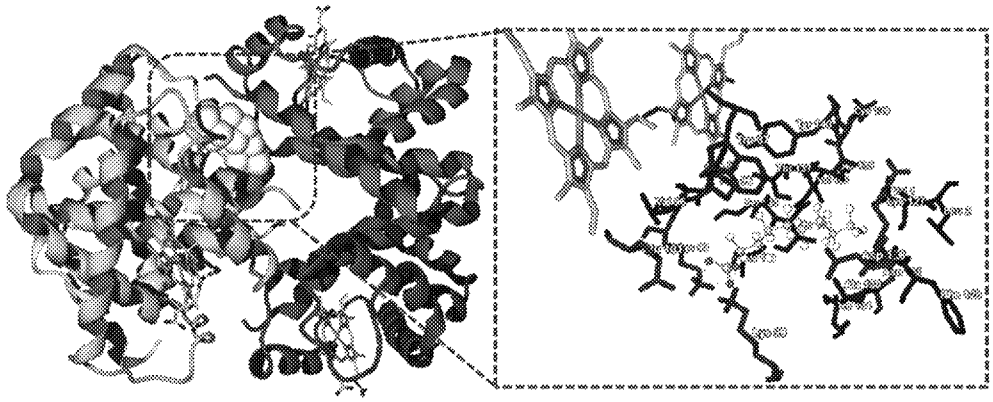

Fig. 11. Predicted orientation of the lowest docking energy conformation of PFOS with Hb. The binding site was enlarged to show the interactions of PFOS with Hb.

shows, the presence of PFOS induced a significant loss of signal in heme group region, implying that PFOS induced the unfolding of the hemoproteins accompanied by exposure of the heme pocket and Hb did undergo significant changes in the heme group symmetry (quaternary structure) and tertiary structure by PFOS binding [25,39]. This conclusion is consistent with the result from UV–vis spectral data, the normal biological function of Hb in transferring oxygen could be effected by the binding interaction of PFOS with Hb.

3.4. The putative binding sites of PFOS on Hb

Molecular modeling is becoming an important method to analyze the intermolecular interactions of protein with PFOS [40]. Herein, structure and energies of the binding sites of PFOS to Hb were determined through molecular modeling. From the docking calculation, the best binding site with minimum binding energy is selected from the minimum energy conformers from 100 runs. In this report, cluster analyses were also performed for the binding sites of PFOS on Hb. A total of 44 multimember conformational clusters were obtained from 100 docking runs. Analyzing from the docking data, we can find that Hb had not only one possible binding site to bind with PFOS. The interaction free energies and reaction energies including ΔG (the estimated free energy of binding energy), $E_{inter\text{-}mol}$ (the final intermolecular energy), E_{VHD} (VDW + Hbond + desolvo energy), E_{elec} (the electrostatic energy), E_{total} (the final total internal energy), $E_{torsional}$ (the torsional free energy) were then calculated for all the binding sites and are summarized in Table 3. As data show, E_{VHD} energy including van der Waals energy (E_{VDW}), E_{Hbond} and $E_{desolvo}$ and E_{elec} are the main part of binding free energies of PFOS with Hb. The predicated binding model with the lowest docking energy was then used for binding orientation analysis (Fig. 11). It indicated that PFOS entered into the cavity of Hb and there were twenty three amino acid residues coming from α1, α2, and β2 subunit that took part in the binding interactions of Hb with PFOS. These amino acid residues are α1Pro-95, α1Val-96, α1Lys-99, α1Ala-130, α1Phe-98, α1Ser-133, α1Thr-134, α1Thr-140, α1Val-135, α1Lys-139, α1Ser-138, α1Tyr-140, α2Lys-199, α2Ala-130, α2Asp-126, α2Lys-127, α2Val-1, α2Leu-2, α2Asn-131, α2Thr-134, α2Phe-128, β2Trp-37, and β2Glu-101. The hydrophobic core of this site is able to host the fluorinated carbon chain while the charge amino interacts with the charged polar head of PFOS. Among above amino residues, Leu, Pro, Val and Phe residues were hydrophobic amino residues, the aromatic amino acid residues including Trp, Tyr and Phe residues were also involved in the binding interaction. In addition, the polar interaction and hydrogen bonds existed between two positively charged amino residues Lys-99 and the $-SO_3^-$ groups of PFOS. Therefore, several kind of forces are presumed to take part in the interaction of PFOS with Hb, which include hydrophobic, hydrogen bonds, van der Waals interactions and electrostatic forces.

4. Conclusion

In conclusion, how PFOS affects the structure and stability of Hb has been reported in this work. The features are as follows. First, PFOS acted as a structure destabilizer for Hb to induce the relatively large changes in the stable helical of secondary structure. Second, the presence of PFOS had an enormous capacity for changing the thermal denaturation process of Hb and resulting in the decrease of the thermal stability of protein. Third, Hb did undergo significant changes in the heme group symmetry (quaternary structure) and tertiary structure by PFOS binding. In addition, PFOS could enter into the binding cavity of Hb by many noncovalent interactions including hydrophobic, hydrogen bonds, van der Waals interactions and electrostatic forces. This is the first study that offer a detailed binding mechanism of PFOS with Hb and its effects on the structures of Hb. We believe that the present study will provide important insight into the molecular toxicology of this kind of PFCs.

Acknowledgement

We gratefully acknowledge financial support of the Fund for the National Natural Science Foundation of China (Project No. 21571154, 21201147), the National Natural Science Foundation of Jiangsu Province (Grant No. BK2012671, BK20151296), and the Jiangsu Fundament of "Qilan Project" and "333 Project", and the sponsorship of *Jiangsu Overseas Research & Training Proggram for University Prominent Young & Middle-aged Teachers and Presidents.*

Transparency document

Transparency document related to this article can be found online at http://dx.doi.org/10.1016/j.cbi.2016.05.019.

References

[1] Q. Huang, Y. Chen, Y. Chi, Y. Lin, H. Zhang, C. Fang, S. Dong, Immunotoxic effects of perfluorooctane sulfonate and di(2-ethylhexyl) phthalate on the marine fish Oryzias melastigma, Fish Shellfish Immunol. 44 (2015) 302–306.
[2] Q.F. Qin, R.T. Liu, X.R. Pan, X.Y. Fang, Y. Mou, Impact of carbon chain length on binding of perfluoroalkyl acid to bovine serum albumin determined by spectroscopic methods, J. Agric. Food. Chem. 58 (2010) 5561–5567.
[3] R. Renner, Perfluorinated sources outside and inside, Environ. Sci. Technol. 38 (2004) 80A.
[4] Y.G. Zhao, H.T. Wan, A.Y.S. Law, X. Wei, Y.Q. Huang, J.P. Giesy, M.H. Wong,

C.K.C. Wong, Risk assessment for human consumption of perfluorinated compound-contaminated freshwater and marine fish from Hong Kong and Xiamen, Chemosphere 85 (2011) 277–283.
[5] L.W.Y. Yeung, Y. Miyake, S. Taniyasu, Y. Wang, H.X. Yu, M.K. So, Y.N. Wu, J.G. Li, J.P. Giesy, N. Yamashita, P.K.S. Lam, Perfluorinated compounds and total and extractable organic fluorine in human blood samples from China, Environ. Sci. Technol. 42 (2008) 8140–8145.
[6] EFSA, Perfluorooctane sulfonate (PFOS), perfluorooctanoic acid (PFOA) and their salts. Scientific opinion of the panel on contaminants in the food chain, EFSA J. 653 (2008), 1–131.
[7] F. Fabrega, V. Kumar, M. Schuhmacher, J.L. Domingo, M. Nadal, PBPK modeling for PFOS and PFOA: validation with human experimental data, Toxic. Lett. 230 (2014) 244–251.
[8] G.W. Olsen, J.M. Burris, D.J. Ehresman, J.W. Froehlich, A.M. Seacat, Half-life of serum elimination of perfluorooctane sulfonate, perfluorohexane sulfonate, and perfluorooctanoate in retired fluorochemical production workers, Environ. Health. Perspect. 115 (2007) 1298–1305.
[9] European Commission, Directive 2013/39/EU of the European Parliament and of the Council of 12 August 2013 amending directives 2000/60/EC and 2008/105/EC as regarding priority substances in the field of water policy, Off. J. Eur. Union (2013) L226I–L22617.
[10] S.C. Chang, P.E. Noker, G.S. Gorman, S.J. Gibson, J.A. Hart, D.J. Ehresman, J.L. Butenhoff, Comparative pharmacokinetics of perfluorooctanesulfonate (PFOS) in rats, mice, and monkeys, Reprod. Toxicol. 33 (2012) 428–440.
[11] L. Zhang, Y.Y. Li, H.C. Zeng, M. Li, Y.J. Wan, H.J. Schluesener, Z.Y. Zhang, S.Q. Xu, Perfluorooctane sulfonate induces apoptosis in N9 microglial cell line, Int. J. Toxicol. 30 (2010) 207–215.
[12] G. Ding, L. Wang, J. Zhang, Y. Wei, L. Wei, Y. Li, M. Shao, D. Xiong, Toxicity and DNA methylation changes induced by perfluorooctane sulfonate (PFOS) in sea urchin Glyptocidaris crenularis, Chemosphere 128 (2015) 225–230.
[13] W. Hu, P.D. Jones, W. DeCoen, L. King, P. Fraker, J. Newsted, J.P. Giesy, Alterations in cell membrane properties caused by perfluorinated compounds, Comp. Biochem. Physiol. Part C. Toxicol. Pharmacol. 135 (2003) 77–88.
[14] F. Hoppe-Seyler, Über die oxydation in lebendem blute, Med-chem Untersuch Lab 1 (1866) 133–140.
[15] M.F. Perutz, Structure of haemoglobin, Brookhaven Symp. Biol. 13 (1960) 165–183.
[16] R. Gabbianelli, A.M. Santroni, D. Fedeli, A. Kantar, G. Falcioni, Antioxidant activities of different hemoglobin derivatives, Biophys. Res. Commun. 242 (1998) 560–564.
[17] M. Paulami, T. Ganguly, Fluorescence spectroscopic characterization of the interaction of human adult hemoglobin and two isatins, 1-methylisatin and 1-phenylisatin: a comparative study, J. Phys. Chem. B 113 (2009) 14904–14913.
[18] N.H. Lu, J.Y. Li, X.M. Ren, R. Tian, Y.Y. Peng, Nitric attenuated hypochlorous acid-mediated heme degradation in hemoglobin, Chem. Biol. Interact. 238 (2015) 25–32.
[19] P.M. Vacek, R.J. Albertini, R.J. Sram, P. Upton, J.A. Swenberg, Hemoglobin adducts in 1,3-butadiene exposed Czech workers: female–male comparisons, Chem. Biol. Interact. 188 (2010) 668–676.
[20] L. Gebicka, E. Banasiak, Interactions of anionic surfactants with methemoglobin, Colloids Surfaces B 83 (2011) 116–121.
[21] P.S. Santiago, F.A.O. Carvalho, M.M. Domingues, J.W.P. Carvalho, N.C. Santos, M. Tabak, Isoelectric point determination for glossoscolex paulistus extracellular hemoglobin: oligomeric stability in acidic pH and relevance to protein–surfactant interactions, Langmuir 26 (2010) 9794–9801.
[22] V.K. Thilakarathne, V.A. Briand, R.M. Kasi, C.V. Kumar, Tuning Hemoglobin–poly(acrylic acid) interactions by controlled chemical modification with triethylenetetramine, J. Phys. Chem. B 116 (2012) 12783–12792.
[23] G. Sekar, S.T. Kandiyil, A. Sivakumar, A. Mukherjee, N. Chandrasekaran, Binding studies of hydroxylated Multi-Walled carbon nanotubes to hemoglobin, gamma globulin and transferring, J. Photochem. Photobiol. B 153 (2015) 222–232.
[24] L.B. Devi, S.K. Das, A.B. Mandal, Impact of surface functionalization of AgNPs on binding and conformational change of hemoglobin (Hb) and hemolytic behavior, J. Phys. Chem. C 118 (2014) 29739–29749.
[25] P.F. Qi, R.T. Liu, Y.P. Teng, Perfluorodecanoic acid binding to hemoproteins: new insight from spectroscopic studies, J. Agric. Food Chem. 59 (2011) 3246–3252.
[26] http://www.scripps.edu/mb/olson/doc/autodock.
[27] http://www.rcsb.org/pdb/explore/explore.do?structureId=1G09.
[28] M.J. Frisch, G.W. Trucks, H.B. Schlegel, G.E. Scuseria, M.A. Robb, J.R. Cheeseman, G. Scalmani, V. Barone, B. Mennucci, G.A. Petersson, H. Nakatsuji, M. Caricato, X. Li, H.P. Hratchian, A.F. Izmaylov, J. Bloino, G. Zheng, J.L. Sonnenberg, M. Hada, M. Ehara, K. Toyota, R. Fukuda, J. Hasegawa, M. Ishida, T. Nakajima, Y. Honda, O. Kitao, H. Nakai, T. Vreven, J.A. Montgomery Jr., J.E. Peralta, F. Ogliaro, M. Bearpark, J.J. Heyd, E. Brothers, K.N. Kudin, V.N. Staroverov, T. Keith, R. Kobayashi, J. Normand, K. Raghavachari, A. Rendell, J.C. Burant, S.S. Iyengar, J. Tomasi, M. Cossi, N. Rega, J.M. Millam, M. Klene, J.E. Knox, J.B. Cross, V. Bakken, C. Adamo, J. Jaramillo, R. Gomperts, R.E. Stratmann, O. Yazyev, A.J. Austin, R. Cammi, C. Pomelli, J.W. Ochterski, R.L. Martin, K. Morokuma, V.G. Zakrzewski, G.A. Voth, P. Salvador, J.J. Dannenberg, S. Dapprich, A.D. Daniels, O. Farkas, J.B. Foresman, J.V. Ortiz, J. Cioslowski, D.J. Fox, Gaussian 09, Revision D.01, Gaussian Inc., Wallingford, CT. 2013.
[29] http://www.cicbio.com/products/molgro.
[30] D.M. Davis, D. McCloskey, D.J.S. Birch, P.R. Gellert, R.S. Kittlety, R.M. Swart, The fluorescence and circular dichroism of proteins in reverse micelles: application to the photophysics of human serum albumin and -acetyl- tryptophanamide, Biophys. Chem. 60 (1996) 63–77.
[31] H.M. Zhang, K. Liu, J. Cao, Y.Q. Wang, Interaction of a hydrophobic- functionalized PAMAM Dendrimer with Bovine serum albumin: thermodynamic and structural changes, Langmuir 30 (2014) 5536–5544.
[32] N. Samanta, D.D. Mahanta, S. Hazra, G.S. Kumar, R.K. Mitra, Short chain polyethylene glycols unusually assist thermal unfolding of human serum albumin, Biochimie 104 (2014) 81–89.
[33] D. Lucent, V. Vishal, V.S. Pande, Protein folding under confinement: a role for solvent, PNAS 104 (2007) 10430–10434.
[34] W. Pfeil, P.L. Privalov, Thermodynamic investigations of proteins. III. Thermodynamic description of lysozyme, Biophys. Chem. 4 (1976) 33–40.
[35] W. Liu, X. Guo, R. Guo, The interaction between hemoglobin and two surfactants with different charges, Int. J. Biol. Macromol. 41 (2007) 548–557.
[36] W. Liu, X. Guo, R. Guo, The interaction of hemoglobin and hexadecyltrimethylammonium bromide, Int. J. Biol. Macromol. 37 (2005) 232–238.
[37] W.C. Abert, W.M. Gregory, G.S. Allan, The binding interaction of coomassie blue with proteins, Anal. Biochem. 213 (1993) 407–413.
[38] B.M. Zhang, Q.H. Zhou, J. Cao, Y.Q. Wang, Mechanism of cinnamic acid-induced trypsin inhibition: a multi-technique approach, Spectrochim. Acta Part A 116 (2013) 251–257.
[39] F.A.O. Carvalho, F.R. Alves, J.W.P. Carvalho, M. Tabak, Guanidine hydrochloride and urea effects upon thermal stability of Glossoscolex paulistus hemoglobin (HbGp), Intern. J. Biol. Macromol. 74 (2015) 18–28.
[40] S. Matteo, M. Isabella, C. Carlo, Determination of energies and sites of binding of PFOA and PFOS to human serum albumin, J. Phys. Chem. B 114 (2010) 14860–14874.